ACAES systems to enhance the self-consumption rate of renewable electricity in sustainable energy communities

ACAES systems to enhance the self-consumption rate of renewable electricity in sustainable energy communities

Daniele Cocco, Fabio Licheri, Davide Micheletto, Vittorio Tola

Department of Mechanical, Chemical and Materials Engineering
University of Cagliari, Via Marengo 2, 09123 Cagliari, Italy

daniele.cocco@unica.it

Abstract. This paper aims to evaluate the optimal configuration of an Adiabatic Compressed Air Energy Storage (ACAES) system designed to achieve the best matching between power production from non-programmable Renewable Energy Sources (RES) power plants and power demand from final users. The electrical energy demand of a small town, with a maximum power load of about 10 MW, has been considered as case study. The electrical energy can be supplied by both a photovoltaic (PV) power plant and the grid. For the ACAES system, different sizes for compressor, turbine, thermal energy storage (TES) system and air storage reservoir have been evaluated by varying the air mass flow rate of turbomachines and the charging and discharging duration times, to enhance the share of the PV energy supplied to the end user. The best performance is achieved with a PV power plant rated at about 35 MW and an ACAES section characterized by a compressor/turbine rated power of about 25-35% of the maximum power load of the end user, with a charging time of about 10 hours and a discharging time of about 20 hours. The average round-trip efficiency of the ACAES system is around 70%. On the overall, the integrated PV-ACAES system allows to cover 66% of the yearly electrical energy demand.

1. Introduction

One of the main targets of the European Union (EU) directives is the promotion of more sustainable energy communities such as a small town, a small industrial district, etc. The achievement of this goal requires the development of flexible and effective systems to increase the self-production rates of renewable electricity (mainly produced by wind and solar energy) in mini grids. Energy storage systems of medium size storage capacity will play a fundamental role to enhance the self-consumption rate of Renewable Energy Sources (RES) in sustainable energy communities. In recent years, many technologies have been developed for distributed energy storage, each characterized by specific features in terms of maximum deliverable power, storage capacity, round-trip efficiency, lifetime etc. Therefore, each technology is suitable to cover specific applications at the utility scale as demonstrated by many review studies on the state of the art of energy storage technologies [1-3].

Among the energy storage systems characterized by medium-high storage capacities and, therefore, suitable for peak load shaving and/or load levelling tasks, Compressed Air Energy Storage (CAES) systems are one of the most interesting options, potentially more cost-effective compared to batteries and somehow comparable to pumping hydro systems. CAES technology is similar to conventional gas turbine plants, but the compression and expansion processes are deferred in time and thus require a suitable reservoir to store the compressed air. Conventional CAES configurations include a combustion chamber, usually fed by a fossil fuel, for air heating before the expansion phase. However, the more advanced adiabatic CAES (ACAES) configurations reduce or eliminate the fossil fuel consumption by

the introduction of a Thermal Energy Storage (TES) section that allows recovering the thermal energy from the compressed air. Many researchers have investigated different ACAES configurations. For instance, Tola V et al. [4] analysed an ACAES configuration with thermocline thermal energy storage, proposing a compressor control strategy to minimize its off-design behaviour in the charging phase to achieve a round trip efficiency around 75 %. Wang S et al. [5] presented the results of an experimental study on an ACAES plant with thermal energy storage and compared them to the mathematical simulations. The compressors electrical energy was 32.7 % higher than the design value and the output electrical energy was 22.7 % lower than the design value, resulting in an average round trip efficiency of 22.6 %. Guo C et al. [6] proposed a low temperature TES configuration considering part load characteristics of the compressors and the expanders and determined an increase in efficiency after the first three charging and discharging cycles.

Especially for high storage capacity units, the proper siting of the air storage reservoir is the crucial point for the design of CAES systems. However, in many areas of the world there is a widespread availability of geological formations or disused mining cavities, potentially suitable for the storage of compressed air. For this reason, CAES technology is a very interesting storage option and with a high development potential.

Mini-grids powered by RES operate with continuously varying values of produced and required power flows and therefore require flexible energy storage systems. For this reason, in ACAES systems the compressor and the turbine must be able to operate in extremely variable operating conditions. In particular, during both the charging and the discharging phases, the air pressure inside the underground cavity varies continuously and the compression and expansion sections operate with variable values of the compression or expansion ratios. For this reason, the compression and expansion sections are usually based on more than one machine, with different sizes and types. Moreover, according to the requirement to operate with different air mass flow rates and with different values of input and output power, the ACAES systems should be based on variable speed machines. The operation of the TES section is also strongly influenced by the variation of the air mass flow rate and the compressor pressure ratio. To avoid the use of intermediate heat transfer fluids and the introduction of additional heat exchangers, the TES section is typically based on a single-tank packed-bed containing low-cost filling materials.

In recent years, due to the high interest in developing new and efficient energy storage technologies, many research activities have examined the performance of ACAES systems coupled with wind or solar power production plants. Arabkoohsar A et al. [7] proposed a PV plant coupled with a 100 MW_p ACAES storage plant with an ancillary solar collector system. During a one-year period, they found the ACAES plant can increase the efficiency and the reliability of the PV plant and determined a payback time of less than 9 years. Bansal M et al. [8] demonstrated that coupling a PV plant with an ACAES system to supply a constant load is a profitable solution. Chen J et al. [9] analysed the environmental impact of an ACAES plant, deducing that it has a significant benefit on the total emissions compared to coal power production. Marano V et al. [10] studied a conventional CAES configuration, combined with both a wind farm and a photovoltaic plant, in relation to a given power profile demand during a one-day period, demonstrating that the plant can increase the total revenues and reduce CO_2 emissions. Dolatabadi A et al. [11] analysed an optimal scheduling strategy for a PV-CAES system based on a forecasting model, in order to maximize the profitability of the plant. Although the results of these studies are promising, it is necessary to evaluate the off-design performance of the compressors, the dynamic behaviour of the thermal energy storage unit and to assess the performance taking into account the real power load of a reference end user for a year.

In this framework, this paper aims to evaluate the performance of ACAES systems specifically conceived for the integration in mini grids mainly powered by non-programmable RES. In particular, the features and the performance of the main plant components as well as the configurations of the overall ACAES system depend on the power load requirement of the end users and on the power generation profiles of RES power plants. Therefore, the study aims to evaluate the optimal configuration of the ACAES system required to achieve the best matching between power production and consumption and thus the highest level of energy self-consumption.

The electrical energy demand of a little town (about 6000 inhabitants), with a maximum power load of about 10 MW, has been considered as case study. The daily power load profile has been assumed as end user demand. The electrical energy can be supplied by both a photovoltaic (PV) power plant and the grid. Different peak power outputs of the PV power plant, from 25 MW to 45 MW have been considered and compared. To enhance the share of the PV energy supplied to the end users, the introduction of an ACAES system has been considered. In particular, different sizes for compressor, turbine, TES system and air storage reservoir have been evaluated by varying the air mass flow rate and the charging and discharging duration times.

2. System configuration

The power load demand, the plant configuration, the assumptions of ACAES system and the performance of the PV power plant are described in the following.

2.1. End user load demand

To assess the capability of the proposed ACAES plant to meet the energy demand of the end users, the daily power load profile of a small town of about 6000 inhabitants was taken as reference. The available data refer to the power required by the end user for every day of a year, on a quarter-hour base. The overall load is given by the sum of the power required by the different end-users of the town (houses, public buildings, small farms, public lighting, etc.). The power demand varies according to the hour of the day, the day of the week and the month. The peak power registered is around 10.3 MW and the total energy consumption during a year is 48.50 GWh. In Figure 1a, the power load profile (continuous line) of both a typical week-day and a weekend day (dashed line) are shown. It can be observed that the load changes rapidly during the day, with three peaks around 7:00, 13:00 and 21:00. Figure 1b shows the monthly energy demand of the reference town, where it can be observed that the energy consumption is low in the summer months from April to September (except for August), with a minimum of around 3.4 GWh in September, and it is generally high in the winter months from October to March with a maximum of 4.78 GWh in January. The mean monthly energy demand, represented by the dashed line in Figure 1b, is about 4.04 GWh.

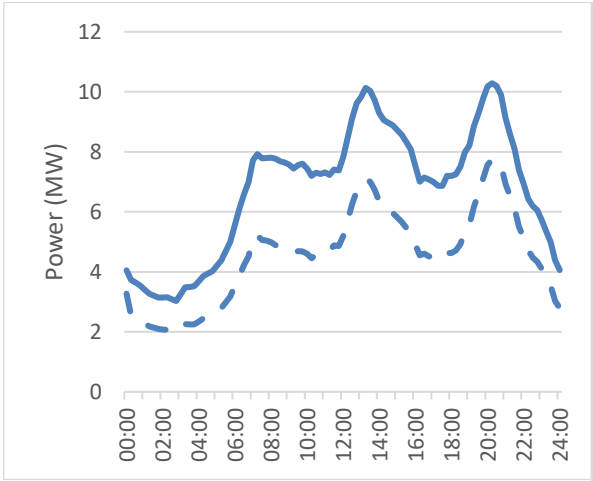

Figure 1a. Load profiles during week and weekend days.

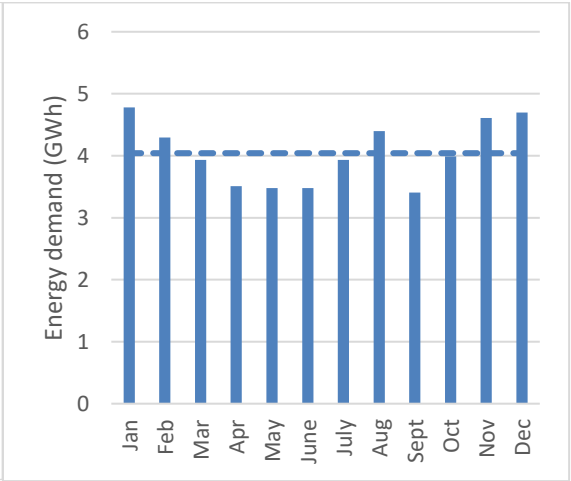

Figure 1b. Monthly energy demand.

2.2. Photovoltaic plant

Compared to conventional diabatic CAES configurations, ACAES plants do not require any fossil fuel combustion as additional energy source. For this reason, this technology matches very well with renewable energy production plants. In this study, the proposed ACAES plant is used to balance the

energy production of a photovoltaic plant specifically designed to produce the energy required by the reference end user.

The rated power output of the PV plant is one of the design parameters to be investigated. The calculation of the expected annual performance has been carried out with reference to a commercial 300 W_p PV panel, with 15.3% conversion efficiency [12]. For the calculation of the expected hourly production of the PV plant, the global solar irradiance (for a surface oriented toward south and with 30° tilt) determined by Meteonorm software [13] for a site in the South-West of Sardinia, was assumed as the main input. According to the specifications of the PV module, the actual operating cell temperature, the PV module efficiency, and the power output are calculated. The hourly power output of the overall PV plant is subsequently calculated by including both inverter efficiency (96%) and secondary losses (93%). For every hour of the year, the power output of each PV module can be calculated and a typical daily power production profile for the summer months (continuous line) and for the winter months (dashed line) of the solar panel is shown in Figure 2a. The electrical energy production of the module, for each month, is shown in Figure 2b.

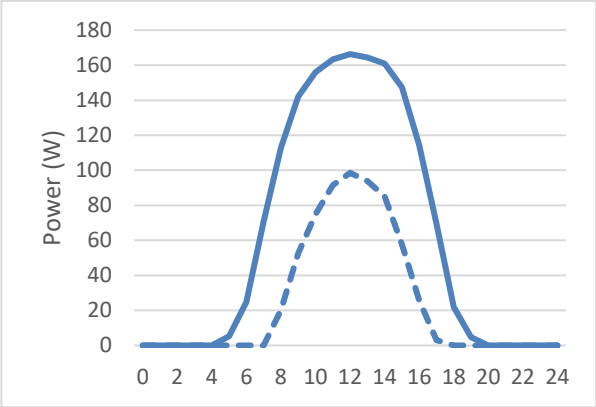

Figure 2a. Power production profiles of a PV module during a summer day and a winter day.

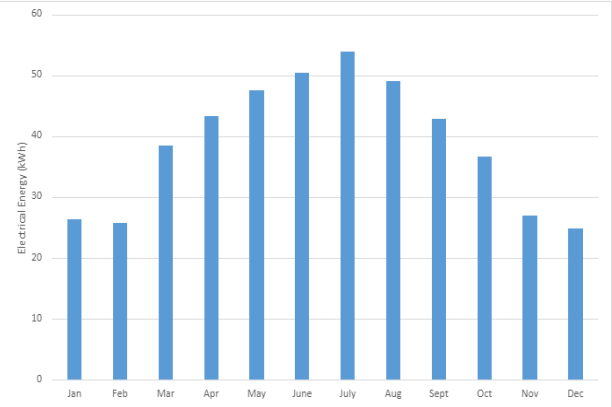

Figure 2b. Monthly energy production of the PV module.

The capacity factor of the PV plant is 16%, which means that the yearly energy production of a 1 MW_p plant is about 1405 MWh. Therefore, according to the annual energy consumption of the town and the expected performance of the ACAES plant, the 5 different sizes of the PV plant listed in Table 1 are considered (configurations C1-C5). In particular, configuration C3 shows a yearly electrical energy production approximately equal to the total energy demand of the end user. Configurations C1 and C2 are characterized by a yearly energy production lower than the yearly energy demand, while configurations C4 and C5 are characterized by a yearly energy production higher than the yearly energy demand. For each configuration, the number of PV modules is given by the ratio of the nominal total power and the peak power of a single module.

Table 1. Configurations of the PV plant considered.

	C1	C2	C3	C4	C5
Power (MW)	25	30	35	40	45
Energy (GWh/year)	35.13	42.16	49.19	56.21	63.24
Number of PV modules	83333	100000	116666	133333	150000

2.3. ACAES configuration

The functional scheme of the proposed ACAES plant is shown in Figure 3. In the first section of the plant, the air is compressed up to 27.6 bar by two compressors: the low pressure one (LPC) and the

medium pressure one (MPC), both driven by the electric motor M1. A thermocline TES unit is used to cool down the compressed air and store the recovered thermal energy. A heat exchanger IC is added at the outlet of the TES to set the temperature to 35 °C before entering the high pressure compressor (HPC), which is driven by the electric motor M2. Finally, the air is cooled down by the aftercooler AC to 35 °C before being stored in the underground cavern. The total energy required for the compression phase is the sum of the electrical energy supplied to the two motors M1 and M2.

During the discharging phase, the air leaving the cavern is heated up by flowing through the TES unit, before expanding in the turbine train, composed by a high-pressure turbine (HPT) and a low-pressure turbine (LPT). The generator G allows the conversion of mechanical energy into electrical energy, which can be supplied to the end user. A throttle valve is used to adjust the air pressure at the inlet of the HPT to the design value of 40 bar.

In this study, the storage volume is obtained from a decommissioned coal mining tunnel, with a diameter of 5 m and located at a depth of about 500 m below the ground level. With these specifications, the cavern is assumed to be suitable for high pressure air storage [14]. It is also assumed that the entire cavern is sealed with state-of-the-art lining, which allows to neglect air leakage [15]. Based on these assumptions, the maximum pressure inside the storage cavern was set to a conservative value of 70 bar.

For a given storage volume, such as the one in this study, the level of charge is expressed as the ratio between the actual pressure of the air inside the cavern and the minimum pressure. During the charging phase, the pressure inside the cavern increases continuously. For this reason, the compressor train operates with a variable pressure ratio and therefore at off-design conditions. To reduce the impact of the off-design operating on the overall efficiency, in the proposed configuration the LPC and the MPC operate at a constant pressure ratio of 12.0 and 2.3 respectively, while the HPC is responsible for the pressure increase in the cavern. By keeping a constant air mass flow rate, the first two compressors can operate at design conditions throughout the entire charging process. In this way, most of the compression work (about 86% of the total) is carried out by the first two compressors at design efficiency, while only a small portion of the total work is affected by the off-design behaviour of the HP compressor. The variation of pressure ratio of the HPC can therefore be achieved by varying the rotational speed at constant mass flow rate. For this reason, the HPC is driven by a dedicated motor M2, whose rotational speed can be adjusted by using an inverter.

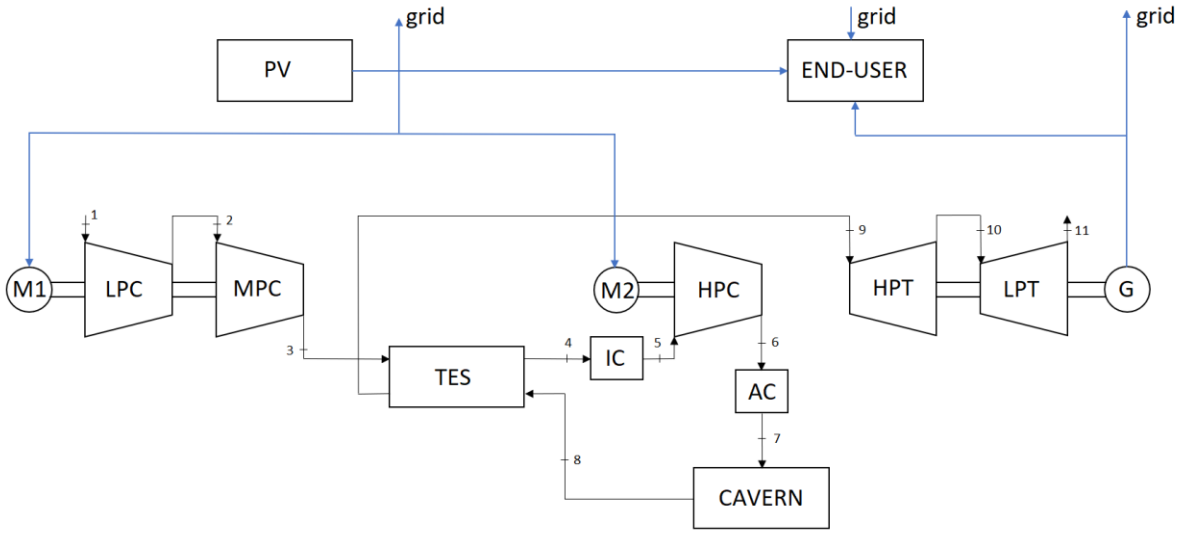

Figure 3. Functional scheme of the proposed ACAES system.

2.2.1 Compression train

As already mentioned, to maximize the overall efficiency of the compression train, most of the work should be carried out by LPC and MPC. According to the current compressor technology, the pressure ratio of the first two compressors was set to reach a maximum temperature of about 600 °C at the outlet

of the MPC. The steadiness of the temperature also leads to a beneficial effect on the behaviour of the thermocline profile of the TES unit, as will be explained in more detail afterwards. All three compressors are multistage centrifugal machines, given the low mass flow rate and the high pressure ratios at which they operate. The design and off-design performance of the three compressors have been estimated by employing the well-known Casey and Robinson method [16]. The LPC is a 6-stage centrifugal compressor with a pressure ratio of 12, while the MPC is a 2-stage centrifugal compressor with a pressure ratio of 2.3 and an air exit temperature of around 598 °C. Because of the higher rotational speed, the MP compressor requires a gear train with a gear ratio of about 3.34.

The HPC is a 2-stage centrifugal compressor, driven directly by the motor M2, with a design pressure ratio of 2.2 and a maximum efficiency of 0.80. As already mentioned, this compressor operates with a variable pressure ratio. Figure 4 shows the maps of this compressor, in terms of pressure ratio (4a) and efficiency (4b) as a function of mass flow rate and rotational speed, while the blue circle indicates the design point. For a given mass flow rate, to increase the pressure ratio, the rotational speed must change accordingly. Values of the rotational speed ranging between 70 % and 110 % of the reference value are reported in Figure. Figure 4 shows also that by decreasing the pressure ratio, and therefore by reducing the rotational speed, the efficiency decreases significantly. For this reason, the minimum pressure ratio of the HPC, and therefore the minimum air pressure inside the cavern cannot be too low. Based on preliminary calculations, the minimum pressure was set to 40 bar. According to the pressure ratio, the HPC outlet air temperature varies from 97 °C to 167 °C. To enhance the air storage capacity of the cavern, the aftercooler AC is used to reduce the temperature of the air to 35 °C. The main parameters of the MP, LP and HP compressors are listed in Table 2.

Table 2. Main performance of the LP, MP and HP compressors.

	LPC	MPC	HPC
Pressure ratio	12	2.3	1.45-2.54
N° of stages	6	2	2
Outlet pressure (bar)	12.0	27.6	40.0-70.0
Outlet temperature (°C)	397.0	597.8	96.8-167.2
Polytropic efficiency	0.84	0.86	0.62-0.80

2.2.2 Thermal Energy Storage unit

At the outlet of the MPC, a thermocline TES unit is used to cool down the air to 35 °C, before entering the last stage of compression and store its thermal energy. The stored energy is subsequently used to heat up the air during the discharging phase.

The TES unit consists of a cylindrical tank filled with a packed bed of solid material. In this study, gravel was chosen as filling material because of its low cost and high availability. When the air flows through the bed, it transfers thermal energy to the filling material which increases its temperature according to a thermocline profile. Because of the cyclic operation of the ACAES, the TES system is continuously heated up and cooled down during charging and discharging phases, respectively. Cycle by cycle, the total energy stored in the TES tank decreases in accordance with the behaviour of the thermocline, until it reaches a steady-state condition [17].

The aspect ratio (AR) of the TES, which is defined as the ratio of the axial length to the diameter of the cylindrical tank, is one of the most important design parameters. In case of high AR values, the TES outlet temperature (section 4 of Figure 1) can be kept low, but many cycles are required before reaching the steady-state condition; conversely, in case of low AR values, the outlet temperature is quite high, but the steady-state condition can be reached very rapidly. To achieve a low temperature at the TES outlet and a small number of cycles before saturation, an aspect ratio of 2.5 was chosen. The main parameters of both the TES unit and its filling material are summarized in Table 3.

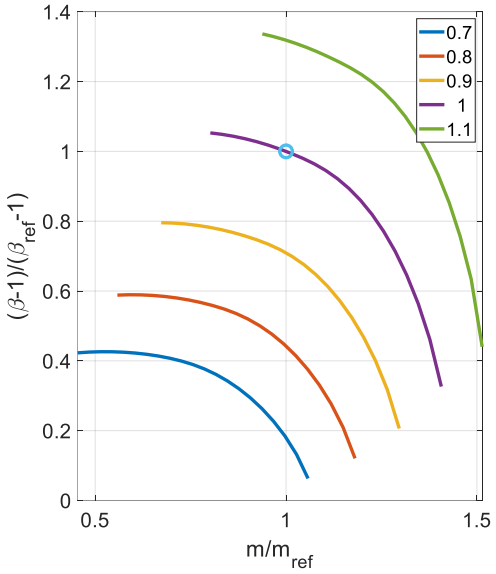

Figure 4a. Generalized pressure ratio of HPC as a function of the generalized mass flow rate.

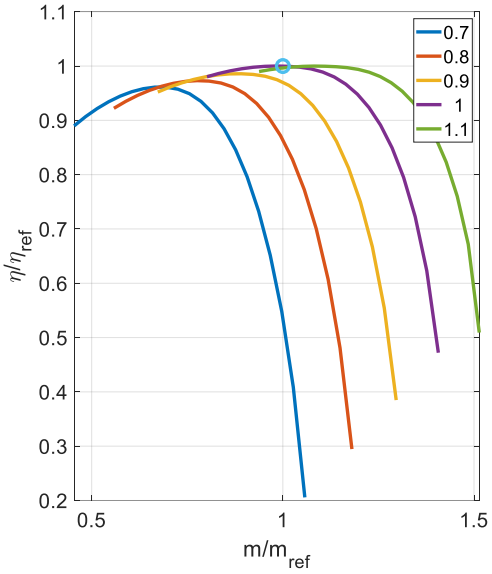

Figure 4b. Generalized efficiency of HPC as a function of the generalized mass flow rate.

Table 3. Main operating parameters of the TES unit.

AR	Inlet temperature (°C)	Design outlet temperature (°C)	Particle diameter (m)	Void fraction	Density (kg/m^3)	Specific heat capacity (J/kgK)
2.5	597.8	35	0.03	0.3	2750	900

2.4. Energy management strategy

The ACAES plant has been modelled on MATLAB/Simulink by solving the mass and energy balances of all plant components and of the overall system for each time step (15 minutes, in this case) of the year. The goal of the ACAES design is to maximize the share of the PV energy production supplied to the end user. Therefore, as shown by Figure 3, the PV plant and the end user are directly connected. When the PV power output is greater than the end user demand, and the storage cavern is not full, the ACAES plant is charged by the surplus energy. Otherwise, the exceeding PV production is sent to the grid. Instead, when the PV power is lower than the end user demand and the level of charge of the cavern is greater than zero, the ACAES plant operates in discharge mode. If the power supplied by the PV and ACAES plants is lower than the overall demand, the remainder is supplied by the grid.

The energy management strategy adopted for this study includes several constraints:

- the maximum time allowed for either charge or discharge was set to 24 hours, so that the ACAES plant must complete a full charge or discharge process in a day or less;
- the charging and discharging processes require minimum power values to start;
- purchasing of electrical energy by the grid for the charging process and selling to the grid during the discharging process was not allowed.

Therefore, the charging process can start only if the available PV power is at least equal to the power required by the compression train. Also, the discharging process can start only when the end user load demand is greater than the PV power plant production. Moreover, according to the available storage volume, the charging and discharging processes may sometimes not be completed and both processes can begin or end at various cavern pressure levels. Furthermore, the interruptions during the charging or discharging processes also influence the thermocline profile inside the TES tank. If the charging process is interrupted before completion, the thermocline profile stops early as well, leading to lower air temperatures, and therefore lower power outputs, during the following discharging phase. Similarly, if

the discharging process cannot be completed, the thermocline profile stops earlier, and a high level of thermal energy is kept in the TES. During the cyclical operation of the ACAES plant, these two phenomena occur frequently, with corresponding worse performance of the TES system, and consequently of the whole plant.

3. Results and discussion

The ACAES plant has been designed to store the exceeding energy produced by the PV plant and therefore the goal of the ACAES design is to maximize the share of the PV energy used by the end user. To find the best ACAES design, the effects of the most important design variables, i.e. PV size, charging mass flow rate, charging and discharging times, have been evaluated.

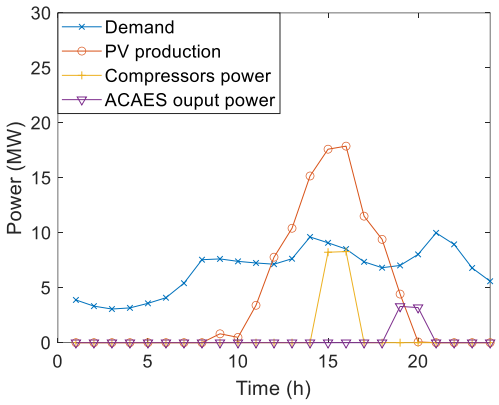

Figure 5a. Power profiles during a typical winter day.

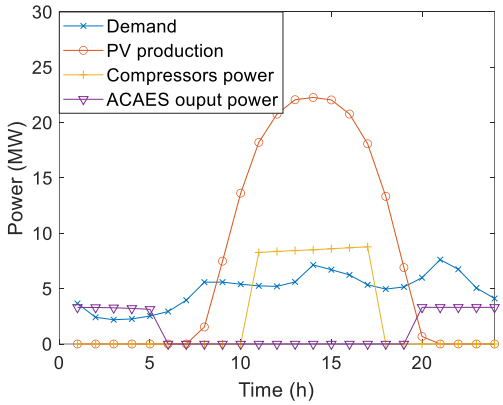

Figure 5b. Power profiles during a typical summer day.

Figure 5a-b shows the main power flows of the PV-ACAES plant for a typical winter day (Figure 5a) and a typical summer day (Figure 5b), with higher values of solar radiation. Both figures refer to configuration C3, and report the PV power production profile, the end user power demand, as well as the input (compressors) and output (turbine) power profile of the ACAES section. Obviously, during summer, the PV system is characterized by higher peak powers and greater energy production in comparison to winter. On the other hand, the energy demand of the end user is generally lower during summer and higher during winter (Figure 1b). These two curves allow to immediately evaluate the direct energy use, the energy surplus, and the energy deficit for the day. It can be observed that the surplus energy produced by the PV plant is much greater in the summer months, with a corresponding higher input power for the ACAES plant. The positive slope of the compressor power curve is due to the increase of the pressure inside the cavern and therefore of the compressors power. The lack of power during the night hours is partially or fully covered by the ACAES power production, represented by the ACAES output power line. During winter, the stored energy only allows to supply electrical energy to the end user for a few hours. Instead, in the summer months the energy demand of the end user can be sustained by the ACAES plant for almost all the night time.

For a given PV size, the ACAES plant can be designed with reference to different values of compressor mass flow rate (and therefore compressor rated power), charging time (and therefore storage volume) and discharge time (and therefore turbine rated power). Figure 6 shows the main yearly energy flows for the ACAES plant as a function of the compressor air mass flow rate. Figure 6 refers to configuration C3, with constant values of charging (11 hours) and discharging (21 hours) times. In particular, Figure 6 shows the total compression energy, the energy supplied to the end user by the ACAES, the energy sent to the grid by the ACAES and the percentage of the demand of the end user supplied by the ACAES plant. Figure 6 demonstrates that all these energy flows increase with the air mass flow rate, that is with the output power of the ACAES plant. However, too high values of the

compressor power reduce the number of hours per year with a sufficient PV power surplus and therefore reduce the operating hours of the compressor train. On the overall, Figure 6 clearly shows the air mass flow rate that maximizes the percentage of the energy demand supplied by the ACAES plant.

Similarly, Figure 7 gives the main yearly energy flows for the ACAES plant as a function of the charging time. Figure 7 refers to configuration C3, with a compressor air mass flow rate of 12 kg/s and a discharging time of 21 hours. Figure 7 shows that all the energy flows increase with the charging time, that is with air storage volume. However, beyond a given charging time, the energy used by the compression train remains almost constant due to the insufficient availability of PV power. In this case, the pressure inside the cavern is often lower than the maximum value, with a corresponding reduction of the energy produced by the turbine. For this reason, Figure 7 clearly shows the charging time that maximizes the percentage of the energy demand supplied by the ACAES plant.

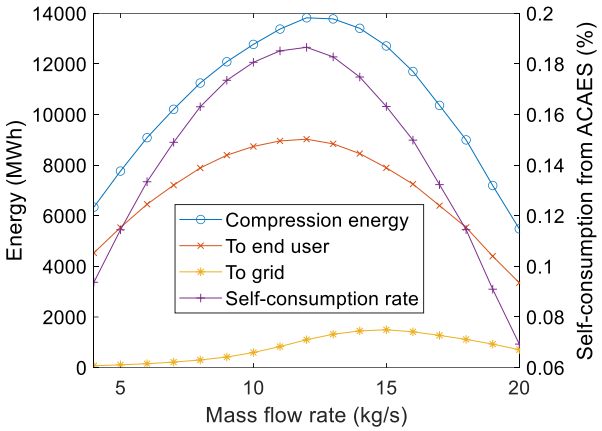

Figure 6. Main energy flows as a function of the compressors mass flow rate at constant charge and discharge times.

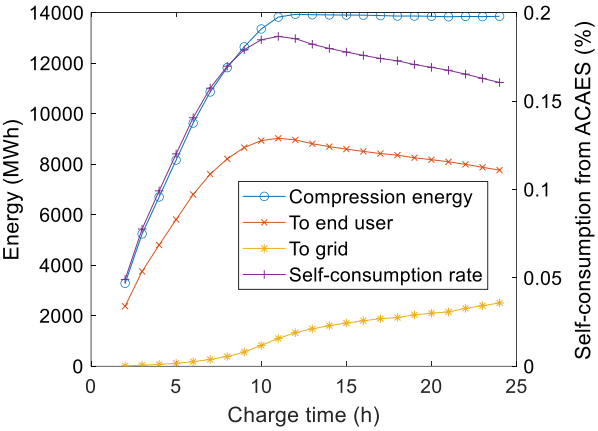

Figure 7. Main energy flows as a function of charge time at constant compressor mass flow rate and discharge time.

Figure 8 gives the main yearly energy flows for the ACAES plant as a function of the discharging time. Figure 8 refers to configuration C3, with a compressor air mass flow rate of 12 kg/s and a charging time of 11 hours. Figure 8 shows that all the energy flows, except for the share of energy sent to the grid, increase with the discharging time, that is with a reduction of the rated power of the turbine. With a short discharge time, the stored energy is released rapidly and at high power; instead, for a long discharge time, energy is released gradually during the night, fulfilling a greater share of the end user demand. Beyond a given discharging time, the energy supplied to the end user remains almost constant, while the energy sent to the grid decreases. This results in a general better utilization of the total electrical energy produced and an increase in the self-consumption rate. On the overall, Figure 8 clearly shows the discharging time that maximizes the percentage of the energy demand supplied by the ACAES plant.

Finally, Figure 9 shows the level of charge in the cavern throughout the year with reference to a compressor mass flow rate of 12 kg/s, a charge time of 11 h and discharge time of 21 h. Figure 9 demonstrates that the charging and discharging processes are often discontinued and depend on both availability and demand of power at every hour of the day. During summer months, the energy production of the PV plant is much greater than the demand of the end user. For this reason, high levels of power are available to the ACAES plant, which can complete the charging process more often. However, most of the end user demand is directly fulfilled by the PV plant and the ACAES plant cannot fully discharge during the night, leaving a medium to high level of pressure inside the cavern. During winter months, the PV plant production is low, and the ACAES plant is required to compensate for the lack of energy. It can be observed that the level of charge in the cavern is often low because the PV plant peak power is insufficient to drive the compressor train until the cavern is fully charged. Furthermore, the input power for the ACAES section is often available only for short times before the demand power profile exceeds the production.

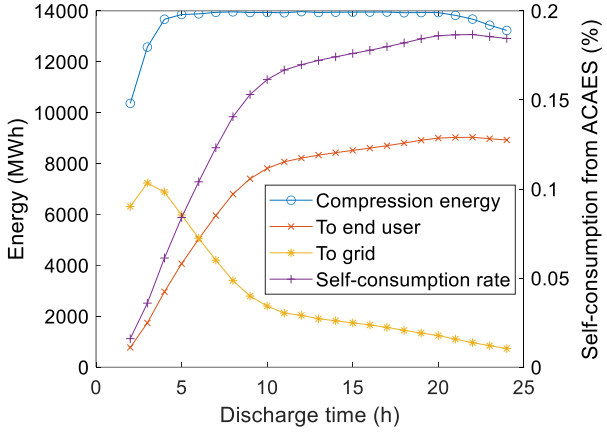

Figure 8. Main energy flows as a function of discharge time at constant compressor mass flow rate and charge time.

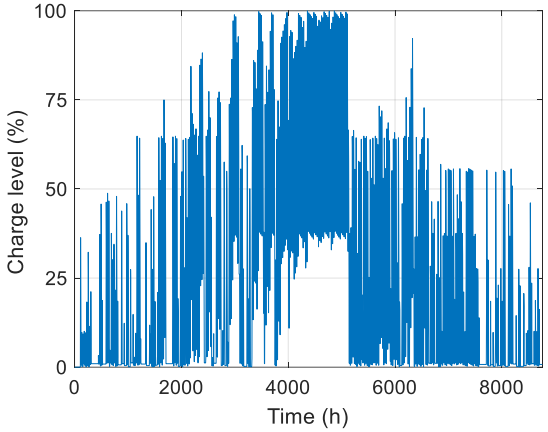

Figure 9. Level of charge inside the cavern during a year.

For each PV configuration, the optimal set of the three design variables, i.e., compressor mass flow rate, charge time and discharge time, was determined, where the objective function is the total electrical energy supplied to the end user. For this optimization problem, to minimize the computation time, the genetic algorithm (GA) included in the MATLAB Optimization Toolbox was used. The results of the optimization problem are listed in Table 4, where for each of the five PV plant configurations the set of parameters that maximize the objective function are reported. From C1 to C5 the optimal charge mass flow rate of the ACAES plant increases due to the higher availability of input power from the PV plant. Since the charge time is approximately half of the discharge time, the discharge mass flow rate is about half of the charge mass flow rate.

Table 4. Optimal design variables for each PV plant configuration.

	C1	C2	C3	C4	C5
Mass flow rate (kg/s)	7	9	12	13	15
Charge time (h)	11	11	11	12	13
Discharge time (h)	21	20	21	22	24

The main performance parameters of the ACAES plant are listed in Table 5. As the PV plant's production increases from C1 to C5, the energy provided directly to the end user increases slightly from around 21.6 GWh/year to around 23.7 GWh/year and the percentage of fulfilled demand increases from 44.65 % to 48.97 %.

4. Conclusion

In this paper, the performance of an ACAES system designed to enhance the energy supply of a PV power plant for a small town of about 5000-6000 people was analysed. First, the end user load profile was characterized for a reference year on a quarter-hour basis. The total energy demand was calculated to be slightly lower than 49 GWh/year with a peak power demand of around 10.3 MW. Then, five configurations of a PV power production plant were analysed to supply energy to the end user, with nominal power ranging from 25 MW to 45 MW. Based on the known forecast for a reference year, the power production profile was defined for each plant's configuration. Based on the interaction between the two power profiles, an Adiabatic-CAES plant with thermocline TES was then proposed to store and then utilize the excess energy produced. The off-design behaviour of the compressors and the daily variation of the thermocline profile of the TES were considered. By keeping the inlet mass flow rate fixed, most of the compression work is carried out at design conditions, allowing to reach a round-trip efficiency of the plant of around 73 %.

Table 5. Main performance parameters of the PV-ACAES plant in the 5 configurations studied.

	C1	C2	C3	C4	C5
Compressors power (MW)	5.2	6.6	8.85	9.6	11.1
Turbines power (MW)	2.0	2.7	3.4	3.8	4.4
Energy demand of the end user (MWh/year)	26845	26046	25481	25068	24748
Compression energy (MWh/year)	7081	10450	13894	16874	20026
Electrical energy production of ACAES (MWh/year)	5233	7699	10174	12342	14637
Electrical energy to the end user (MWh/year)	5012	7239	9090	10566	11796
Electrical energy to the grid (MWh/year)	221	460	1084	1776	2841
Round trip efficiency (%)	73.9	73.7	73.2	73.1	73.1
Energy supplied by the PV (%)	44.65	46.30	47.46	48.31	48.97
Energy supplied by the ACAES (%)	10.33	14.93	18.74	21.79	24.32
Energy supplied by PV-CAES (%)	54.98	61.23	66.20	70.10	73.29

For each of the five PV plant configurations, an optimal set of design variables for the ACAES plant was found, with the goal of maximizing the energy output to the end user. It was determined that the energy utilization in the span of a year can increase significantly with the introduction of an ACAES plant. In fact, for a PV plant with a total electrical energy output approximately equal to the total demand, a PV-CAES plant can supply up to around 66 % of the energy demand of the end user.

References

[1] Kousksou T, Bruel P, Jamil A, el Rhafiki T and Zeraouli Y 2014 Energy storage: Applications and challenges *Solar Energy Materials and Solar Cells* **120** 59–80
[2] Ould Amrouche S, Rekioua D, Rekioua T and Bacha S 2016 Overview of energy storage in renewable energy systems *International Journal of Hydrogen Energy* **41** 20914–27
[3] Johnson S C, Papageorgiou D J, Harper M R, Rhodes J D, Hanson K and Webber M E 2021 The economic and reliability impacts of grid-scale storage in a high penetration renewable energy system *Advances in Applied Energy* **3**
[4] Tola V, Meloni V, Spadaccini F and Cau G 2017 Performance assessment of Adiabatic Compressed Air Energy Storage (A-CAES) power plants integrated with packed-bed thermocline storage systems *Energy Conversion and Management* **151** 343–56
[5] Wang S, Zhang X, Yang L, Zhou Y and Wang J 2016 Experimental study of compressed air energy storage system with thermal energy storage *Energy* **103** 182–91
[6] Guo C, Xu Y, Guo H, Zhang X, Lin X, Wang L, Zhang Y and Chen H 2019 Comprehensive exergy analysis of the dynamic process of compressed air energy storage system with low-temperature thermal energy storage *Applied Thermal Engineering* **147** 684–93
[7] Arabkoohsar A, Machado L, Farzaneh-Gord M and Koury R N N 2015 Thermo-economic analysis and sizing of a PV plant equipped with a compressed air energy storage system *Renewable Energy* **83** 491–509
[8] Bansal M, Dhillon J and Virmani R 2016 Development of operation strategy for a solar PV-CAES based system in market scenario *Proceedings - 2016 2nd International Conference on Computational Intelligence and Communication Technology, CICT 2016* (Institute of Electrical and Electronics Engineers Inc.) pp 362–5
[9] Chen J, Liu W, Jiang D, Zhang J, Ren S, Li L, Li X and Shi X 2017 Preliminary investigation on the feasibility of a clean CAES system coupled with wind and solar energy in China *Energy* **127** 462–78
[10] Marano V, Rizzo G and Tiano F A 2012 Application of dynamic programming to the optimal management of a hybrid power plant with wind turbines, photovoltaic panels and compressed air energy storage *Applied Energy* **97** 849–59

[11] Dolatabadi A, Abdeltawab H H and Mohamed Y A-R I 2022 Deep Reinforcement Learning-Based Self-scheduling Strategy for a CAES-PV System Using Accurate Sky Images-based Forecasting *IEEE Transactions on Power Systems* 1–1
[12] Sunerg Solar Energy *XM 72/156 300Wp https://www.sunergsolar.com/it/ (accessed June 2021)*
[13] Meteonorm Software n.d. https://meteonorm.com/en/ (accessed May, 2022).
[14] Mehta B R and Spencer D 1988 Siting compressed-air energy plants *Tunnelling and Underground Space Technology* **3** 295–9
[15] Okuno T, Wakabayashi N, Niimi K, Kurihara Y and Iwano M 2009 Advanced natural gas storage system and verification tests of lined rock cavern-ANGAS project in Japan *International Journal of the JCRM* **5** 95–102
[16] Casey M and Robinson C 2012 A Method to Estimate the Performance Map of a Centrifugal Compressor Stage *Journal of Turbomachinery* **135**
[17] Cascetta M, Cau G, Puddu P and Serra F 2014 Numerical investigation of a packed bed thermal energy storage system with different heat transfer fluids *Energy Procedia* vol 45 (Elsevier Ltd) pp 598–607